The role of radical and vibrationally excited species for NH_3 formation by plasma catalysis

B. Bayer[1], S. Raskar[2], I. Adamovich[2], A. Bhan[1], and P. Bruggeman[3]

[1] *Department of Chemical Engineering and Materials Science, University of Minnesota, Minneapolis, MN, USA*
[2] *Department of Mechanical and Aerospace Engineering, The Ohio State University, Columbus, OH, USA*
[3] *Department of Mechanical Engineering, University of Minnesota, Minneapolis, MN, USA*

Abstract: In this contribution, we report measurements of radical (N, H) and vibrationally excited species (N_2(v)) in a radiofrequency (RF)-driven atmospheric pressure plasma jet by molecular beam mass spectrometry (MBMS) and investigate the reactivity of these species for NH_3 formation by plasma catalysis. Findings demonstrate that surface-mediated reactions involving N are responsible for NH_3 formation. N_2(v), though present in densities over 100× greater than the N density, is primarily consumed by surface-mediated vibrational relaxation.

Keywords: plasma catalysis, molecular beam mass spectrometry, state-to-state modelling

1. Introduction

Radical and vibrationally excited species produced in nonthermal plasma have the potential to enhance chemical conversion by heterogeneous catalysis. The coupling of nonthermal plasma with heterogeneous catalysis has been shown to synergistically enhance NH_3 formation beyond formation of NH_3 from plasma or catalysis alone. Models suggest that radical (N, H) or vibrationally excited species (N_2(v)) may be responsible for the observed synergy [1-2], although the abundance and reactivity of plasma-derived species have not been experimentally assessed to determine dominant plasma-produced gas phase species and their role in NH_3 formation.

Here, we use molecular beam mass spectrometry to enumerate densities of plasma-derived gas-phase species (N, H, and N_2(v)) in the afterglow of a RF-driven atmospheric pressure plasma jet and assess their ability to form NH_3 through surface-mediated, catalytic reactions over a packed bed of Fe, Ni, or Ag metal wools. Through correlation of consumption of the reactive species in the packed bed with NH_3 formation, we determine that surface-mediated reactions involving N radicals are responsible for NH_3 formation and that H is necessary to selectively produce NH_3 from N over Fe, Ni, and Ag. Although N_2(v) is the dominantly produced species by the plasma jet, no NH_3 formation is observed from N_2(v). Experimentally measured loss of N_2(v) instead can be explained by surface-mediated vibrational relaxation.

2. Methods

A RF-driven atmospheric pressure plasma jet (OD = 3 mm, ID = 2 mm) is used to produce N, H, and N_2(v) and transport these species to a packed bed of Fe, Ni, or Ag wools (~70 µm thickness by SEM, 0.9-2.3 cm^2 surface area per cm reactor). The RF jet is driven at 12.8 MHz, has an inlet composition ranging from 0.1-5% N_2, 0.1-4% H_2 in Ar, average power between 0.8-3.1 W, flow rate between 16.7-66.7 cm^3 s^{-1}, and two modulation cycles, a shorter at 20 kHz with a 50% duty cycle and a longer at 50 Hz with a 50% duty cycle.

The method to measure changes in species densities is visually displayed in Figure 1. MBMS measurements are made with a distance of 5 or 7-15mm from the end of the ground electrode to the end of the quartz tube. In the second configuration, catalyst was packed from 5 mm from the end of the ground to the end of the quartz tube. Species densities measured in the first configuration are representative of species densities at the inlet of the catalyst bed, and species densities measured in the second configuration are representative of species densities at the outlet of the catalyst bed. This allows determination of pathways for NH_3 formation through correlation of consumption of plasma-derived species with NH_3 formation. Gas residence time from the plasma to the catalyst bed is below 1 ms to allow significant transport of reactive species to the catalyst, and gas residence time in the catalyst bed ranges from below 100 µs to 2 ms to allow for measurable consumption of reactive species in the catalyst bed.

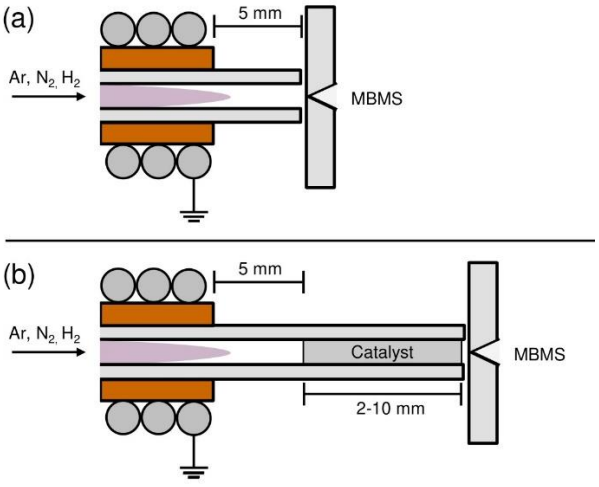

Fig. 1. Plasma jet with and without catalytic bed used to measure species densities at the (a) inlet and (b) outlet of the packed bed of metal wool catalyst.

MBMS is used to measure densities of reactive species. Methods used for detection of species, background subtraction, and absolute species densities calibration are described in more detail by Jiang et al. [3-4].

Vibrational state-to-state kinetic modelling is used to simulate production of $N_2(v)$ by the plasma jet and loss of $N_2(v)$ from gas-phase and surface reactions. Briefly, the quasi-zero-dimensional model simultaneously solves the electron energy equation, the heavy species energy equation, and equations for the species concentrations. Details behind the formulation of the model are described in more detail by Richards et al. [5] and Yang et al. [6].

3. Results and Discussion

3.1 NH_3 formation from plasma-derived species

Measurement of species densities in the configuration of Figure 1(a) demonstrates that measurable densities of N, H, $N_2(v)$, and NH_3 are transported to the catalyst bed. N density ranges between 5.7×10^{13} cm^{-3} to 8.1×10^{14} cm^{-3}, H density from $< 10^{15}$ cm^{-3} to 1.6×10^{16} cm^{-3}, and NH_3 from 6.4×10^{13} cm^{-3} to 6.4×10^{14} cm^{-3} through variation in the inlet composition (% N_2 and % H_2) and power of the plasma jet. Densities of $N_2(v)$ are at least an order of magnitude larger than the N density, with quantification of individual vibrational levels discussed more in section 3.2. Densities of $NH_{x=1,2}$ and $N_2H_{y=1-4}$ species are below the detection limit of MBMS, which is around 10^{13} cm^{-3}.

Experiments that compare N density, NH_3 density, and $N_2(v)$ signal measured in the configuration of Figure (a) or (b) with and without catalyst demonstrate that the presence of catalyst enhances conversion of N and $N_2(v)$ and promotes NH_3 formation, demonstrating that surface reactions involving these species produce NH_3. Figure 2(a) displays a 1:1 correlation between consumption of N (N density at the inlet minus outlet of the catalyst bed) with formation of NH_3 (NH_3 density at the outlet minus inlet of the catalyst bed) over Ni and Ag when H:N > 3 and % H_2 ≥ 0.5 and Fe when H:N > 45 and % H_2 ≥ 2.5. This correlation illustrates that surface reactions involving N are responsible for NH_3 formation at these operating conditions. Experiments that react N and H_2 in absence of H, enabled by a reactor setup that feeds Ar/N_2 through the plasma jet and H_2 after the plasma jet, demonstrate diminished NH_3 formation from N, indicating that H is necessary to form NH_3 from N at the investigated operating conditions.

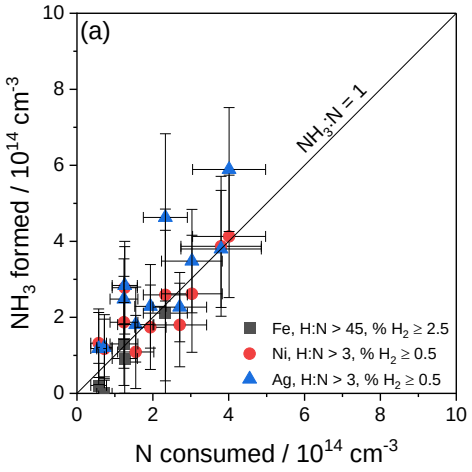

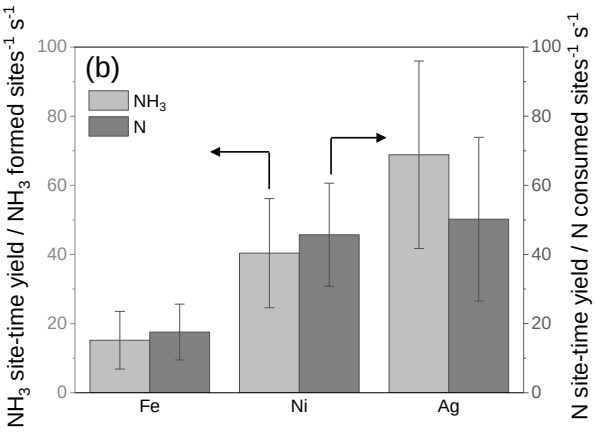

Fig. 2. (a) Correlation between quantities of NH_3 formed and N consumed over Fe, Ni, and Ag for a range of process conditions described in the methods section. (b) Comparison between site-time yields for NH_3 formation and N consumption over Fe, Ni, and Ag. 5% N_2, 0.5% H_2 in Ar, 3.1 W, 66.7 cm^3 s^{-1}

Timescales for N consumption and NH_3 formation are investigated by decreasing the gas residence time in the reactor through increasing the gas flow rate and decreasing the length of the catalyst bed such that N density at the outlet of the catalyst bed is measurable by MBMS. Figure 2(b) compares site-time yields for consumption of N and formation of NH_3, which is the change in density divided by the number of exposed metal surface sites and residence time in the reactor. Within error, the site-time yields for NH_3 formation are equal to the site-time yields for N consumption over Fe, Ni, and Ag, which further demonstrates that surface reactions involving N are responsible for NH_3 formation at the investigated operating conditions [7].

3.2 Pathways for loss of $N_2(v)$ over catalytic surfaces

Formation of $N_2(v)$ in the plasma jet and pathways for consumption of $N_2(v)$ in the gas phase and on the catalyst surface are investigated to assess the reactivity of $N_2(v)$ for NH_3 formation by plasma catalysis. A comparison between densities of $N_2(v)$ predicted by the kinetic model and the experimentally measured N density at the inlet of the catalyst bed is displayed in Figure 3(a). The distribution of $N_2(v)$ is quantitatively consistent with MBMS measurements below the ionization threshold of ground-state N_2 (Figure 3(b)) as described in more detail by Jiang et al. [3]. The total density of $N_2(v>0)$ is two orders of magnitude larger than the N density, with densities of $N_2(v<9)$ having a density greater than the N density.

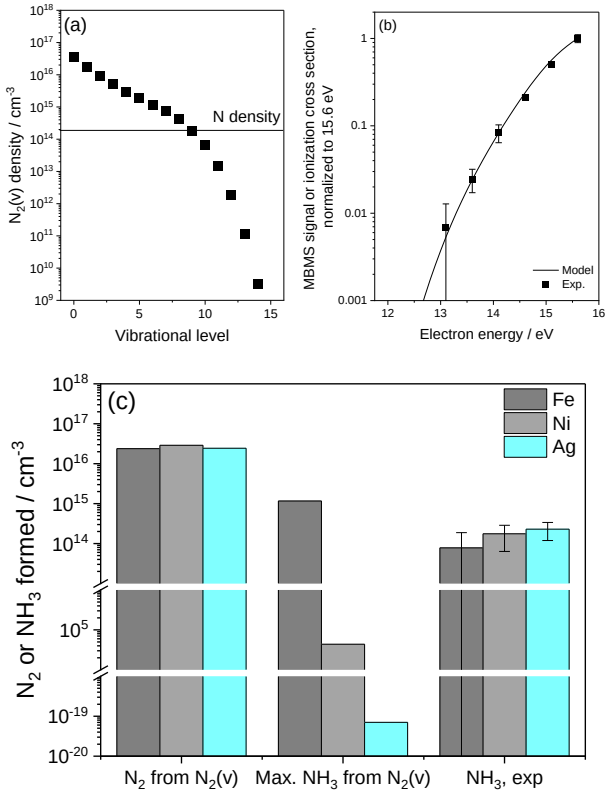

Fig. 3. (a) Densities of $N_2(v)$ at the inlet of the catalyst bed and its comparison to the N density at the inlet (b) Comparison of N_2 formed from $N_2(v)$, max NH_3 formed from $N_2(v)$, and experimentally-observed NH_3 formation over a packed bed of Fe, Ni, and Ag. 0.5% N_2, 0.5% H_2 in Ar, 2.1 W, 16.7 cm^3 s^{-1}

Loss of $N_2(v)$ signal in a 2 mm or 10 mm long empty tube or packed bed of Fe, Ni, or Ag is measured by MBMS. The decrease in $N_2(v)$ signal is larger when the catalyst is present, indicating that surface reactions constitute the dominant loss of $N_2(v)$ for the investigated operating conditions. Experimentally measured loss of $N_2(v)$ corresponds with a kinetic model that describes loss of $N_2(v)$ by surface-mediated vibrational quenching as described by Marinov et al. [8] with a loss coefficient between 0.001-0.0026, which has been measured for loss of $N_2(v)$ over metals by Black et al. [9].

Simulations were performed that consider gas-phase vibrational energy transfer processes, loss of $N_2(v)$ on the surface due to quenching, and maximum rates of NH_3 formation from $N_2(v)$ dissociative adsorption on metal surfaces from Mehta et al. [1] to determine upper bounds on NH_3 formation from $N_2(v)$. Results of these simulations that compare N_2 formation from $N_2(v)$, maximum NH_3 formation from $N_2(v)$, and the experimentally measured NH_3 formation in the packed bed are displayed in Figure 3(c) for densities of $N_2(v)$ at the inlet displayed in Figure 3(a). These simulations show that for all metals, N_2 is produced in quantities at least 10 times larger than NH_3. Over Ni and Ag, the maximum possible NH_3 formation from $N_2(v)$ is orders of magnitude lower than the observed NH_3 formation, indicating that $N_2(v)$ dissociates too slowly to produce NH_3 in quantities greater than NH_3 production from N over these metals. For Fe, the maximum possible NH_3 formation exceeds the experimentally measured NH_3 formation, indicating that $N_2(v)$ could dissociate fast enough to exceed NH_3 formation from N, although assumptions about the surface coverage, rate determining reaction, and other species necessary for NH_3 formation (e.g. H) used in the simulation seem to underpredict additional limitations on possible surface NH_3 formation from $N_2(v)$ over Fe.

4. Conclusion

Investigation of pathways for NH_3 formation from plasma-derived intermediates by plasma catalysis demonstrates that radical species (N, H) react over Fe, Ni, or Ag surfaces to form NH_3. When densities of H_2 and H are sufficient, ~100% of N reacts to form NH_3 over the surfaces. Though $N_2(v)$ is the most abundantly produced plasma-derived species, surface reactions involving $N_2(v)$ do not measurably form NH_3. $N_2(v)$ instead undergoes vibrational relaxation on the surface faster than it reacts to form NH_3 for the investigated operating conditions.

5. Acknowledgements

This material is based upon work supported by the U.S. Department of Energy, Office of Science, Office of Fusion Energy Sciences General Plasma Science program under Award Number DE-SC0020232. The work heavily relied on equipment and methods developed within project DE-SC0001939. SEM-EDS was carried out in the Characterization Facility, University of Minnesota, which receives partial support from the National Science Foundation (NSF) through the MRSEC program.

6. References

[1] P. Mehta et al., Nat. Catal., **1**, 269-275 (2018).
[2] Y. Engelmann et al., ACS Sustainable Chem. Eng., **9**, 39, 13151-13163 (2021).
[3] J. Jiang et al., Plasma Sources Sci. Technol., **31**, 10LT03 (2022).
[4] J. Jiang et al., J. Phys. D: Appl. Phys., **55**, 225206 (2022).
[5] C. Richards et al., Plasma Sources Sci. Technol., **31**, 034001 (2022).
[6] X. Yang et al., Plasma Sources Sci. Technol., **31**, 015017 (2022).
[7] B. Bayer et al., ACS Catal., Accepted.
[8] D. Marinov et al., J. Phys. D: Appl. Phys., **47**, 015203 (2014).
[9] G. Black et al., J. Chem. Phys., **60**, 3526 (1974).